Korean J. Chem. Eng., 35(5), 1119-1127 (2018)
DOI: 10.1007/s11814-018-0010-3

pISSN: 0256-1115
eISSN: 1975-7220

Preparation of corn straw based spongy aerogel for spillage oil capture

Yuan Li*, Xiaodong Liu*, Weijie Cai*, Yafeng Cao*, Yanfeng Sun, and Fengzhi Tan*,†**

*School of Light Industry and Chemical Engineering, Dalian Polytechnic University, Dalian 116034, China
**Zhejiang Ji-Hua Group Co., Ltd., Hangzhou 312368, China
(*Received 3 October 2017 • accepted 25 January 2018*)

Abstract−This work mainly focused on the preparation of a low-cost, ultralight absorbent from renewable corn straw and filter paper via a facile and environmental-friendly approach containing high-shear blending and freeze-drying operation. The physicochemical properties of aerogel were thoroughly examined by several characterization techniques. The satisfactory hydrophobicity of the spongy aerogel was attributed to the formation of polysiloxane on the surface of methyltrimethoxysilane (MTMS) by the silanization reaction. Owing to its superior features, such as ultralow density, high porosity, desirable hydrophobicity, the corn straw based spongy aerogel exhibited a remarkable absorption capacity for both crude oil (36 g/g) and common organic solvents including carbon tetrachloride (CCl_4, 45 g/g), dimethyl sulphoxide (DMSO, 24 g/g), N, N-dumethylformamide (DMF, 45 g/g). This might shed light on the design of efficient adsorbent for oil spills and organic pollutants to meet with the sustainable development.

Keywords: Aerogel, Corn Straw, Filter Paper, Freeze-drying, Oil Absorption

INTRODUCTION

Oil spills and water pollution have attracted much attention because for their disastrous effect on the environment and ecosystem [1]. Considerable efforts have been carried out to remove spilled oil and organic pollutants from water, including burning [2], biodegradation [3], gravity-driven filtration [4], adsorption [5,6], and demulsification [7]. Among these degreasing processes, oil absorbent is considered to be an efficient method considering its low cost, high adsorption capacity and recyclability [8,9]. A series of absorbents such as wool fibers [10], polyurethane sponges [11] and mineral materials [12] have been previously prepared and reported. However, these materials generally had several shortcomings such as low absorption ability, complicated fabrication process, poor buoyancy and less oil/water selectivity, which greatly limited their practical application. Therefore, developing efficient and cheap materials to diminish the pollution of spillage oil is of great importance from the economic and environmental friendly point of view.

Sponges, a common and inexpensive porous material, have a three-dimensional frame structure, which supplies enormous space for oil absorption and storage. Meng et al. [13] prepared a sponge-like carbon aerogel from microfibril cellulose. The highest sorption capacity of aerogel can reach as high as 86 g/g (paraffin oil). Moreover, Khosravi at al. [14] successfully synthesized a highly oleophilic and hydrophobic sponge by polymerization of polypyrrole and a subsequent modification with palmitic acid. Absorbed oils can be collected easily by simple mechanical squeezing of the sponge, because sponge can be compressed repeatedly without collapsing. Unfortunately, these types of sponges mainly come from the non-renewable petroleum-derived products such as poly(melamine-formaldehyde) (PMF), polyurethane (PU) and polystyrene. In contrast, the research of sponge production from renewable biomass is still in its infancy. Cellulose is one of the most abundant natural biomass [15]. Selecting cellulose as a building block to produce 3D porous sponges will be significantly promising. To date, two typical processes to prepare cellulose-derived sponge have been developed [16]. On the one hand, solvable cellulose is made from cellulose derivatives, and then they are dissolved again to prepare cellulose sponge, including cellulose sulfonate method and cellulose carbamate method [17]. Another one was that cellulose is directly dissolved by appropriate solvent. However, the solvents applied in above processes such as N, N-dimethylacetamide (DMAC), N-thylmorpholine-N-oxide (NMMO) and other ionic liquids are too expensive to realize large-scale industrialization [18,19]. In addition, Sun et al. [20] reported a facile and green pathway to produce low-cost and ultralight microcrystalline cellulose fibers (MCFS) from cellulose fibers. MCFS can efficiently absorb oil from an oil-water mixture and the absorption capacity as high as 88-228 times its own weight. More importantly, this type of absorbent presents excellent flexibility and elasticity and can be repeatedly squeezed without structure disruption (more than 30 times).

Natural plants are the most important renewable resources; some natural fibers such as cotton [21], kapok [22] can be used as oil absorbent. As an abundant agricultural residue available worldwide [23], the high-valued application of huge amounts of corn straw is limited. In China, corn straw is burned in situ in many places, thus resulting in serious environmental pollution. Efficient utilization of corn straw resources is essential to resolve air pollution caused by straw burning [24]. Extensive studies on corn straw have been conducted to enhance the value of corn straw such as animal feed, production of paper, biochar [25], xylose [23], ethanol [26], fermentable sugars [27] and absorption materials [24]. Corn

†To whom correspondence should be addressed.
E-mail: tanfz@dlpu.edu.cn, fz_tan@126.com

straw is one of the suitable raw materials to prepare oil absorbent because of its renewability, low-cost, plentifulness and biodegradability. Unfortunately, the flexibility of corn straw based aerogel is not satisfactory for practical application and the materials are too brittle to be widely used. Based on this consideration, it is of great importance to improve the related properties by dopants [28-30] etc. Hence, filter paper fibers have been added by mechanical mixing to enhance the flexibility of the aerogels.

In this work, a series of corn straw/filter paper composite aerogels were synthesized by a facile and low-cost approach. The corn straw can be fully utilized, without the separation of straw skin, core and/or complex pretreatment. The oil absorption capacities of the as-prepared spongy aerogels in various oil/water mixtures were also extensively investigated to elucidate the relationship between the structural property and adsorption capacity. The corn straw based spongy aerogel displayed good stability performance and high absorption capacity, and it could serve as a promising oil-adsorbing material.

MATERIALS AND METHODS

1. Materials

Corn straw was collected from a farm in Dalian (China), then ground into powder, passed through an 80-100 mesh sieve and dried at 80 °C for 24 h. Waste filter paper was obtained from Shanghai Best Biological Technology Co., Ltd. Methyltrimethoxysilane (MTMS, 98%) was purchased from Aladdin Industrial Corporation (Shanghai China). Acetone, dichloromethane, hexane, DMF, ethanol, DMSO and other chemicals were purchased from the Kermel Chemical Reagent Co., Ltd. (Tianjin China). All chemical reagents were of analytical grade and used without further purification. Pump oil, white oil, motor oil and crude oil were supplied by Dalian Petrochemical Company.

2. Pretreatment of the Corn Straw (P-CS)

First, raw corn straw was immersed into a sodium hydroxide aqueous solution (4 wt%) and the ratio of solid-liquid was set as 1 : 15. Then, the mixture was magnetically stirred at 30 °C for 4 h. In the next process, hydrochloric acid was added into above aqueous dispersion until the pH was 7.0. After thorough filtration and washing with deionized water, the obtained corn straw particles (P-CS) were dried at 60 °C for 12 h.

3. Preparation of Oil Absorption Materials (MTA-CS)

Scheme 1 presents the fabrication process of aerogel from P-CS and filter paper.

In detail, the filter papers were cut into small fragments, and then a mixture of P-CS and filter paper was dispersed into deionized water. The mass ratios of P-CS and filter paper were fixed at 1 : 1, 1 : 2, 1 : 3, 2 : 1, 2 : 3, 3 : 1, 3 : 2, then the fiber-to-water mass concentration in aqueous dispersion was controlled within 1 wt%, 1.5 wt%, 2 wt% and 2.5 wt%, respectively. The suspension was subject to vigorous mechanical stirring with a high-shear emulsifying machine (3,000 rpm, 30 min). Thereafter, the as-prepared suspension was frozen at −25 °C for 12 h and freeze-dried at −55 °C (1 mpa) for 36 h to prepare corn straw based spongy aerogel (A-CS).

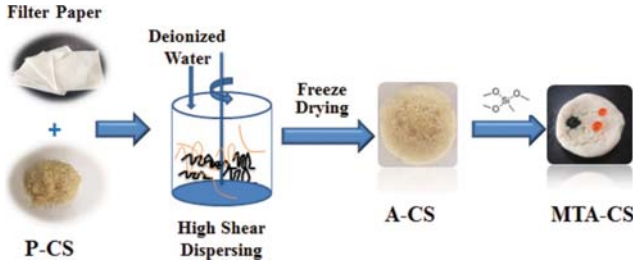

Scheme 1. Fabrication process of corn straw based spongy aerogel.

As reported by Fan et al. [15], the hydrophobicity of A-CS was improved via silanation reaction by chemical vapor deposition (CVD) method. First, 1.5 mL MTMS was mixed with A-CS in reagent bottle. Then the vessel was tightly sealed and placed in an oven at 80 °C for 12 h. The modified sample was taken out and placed in a vacuum oven for 12 h at 60 °C to remove the unreacted MTMS. Thus, the hydrophobic modified corn straw based aerogel (MTA-CS) was obtained.

4. Characterization

Porosity of MTA-CS was calculated as follows:

$$\text{Porosity}\ (\%)=100\times(1-\rho_b/\rho_s) \tag{1}$$

where ρ_b (g·cm^{-3}) is the density of MTA-CS, ρ_s (g·cm^{-3}) is the density for both CS and filter paper considering their similar density, ρ_s=1.528 g·cm^{-3}.

The adsorption capacity of MTA-CS was measured by immersing the aerogel in different solvents (including diesel, ethanol, DMSO, DMF, methanol, toluene, soybean oil and crude oil) for a certain time and then picked out for measurement. MTA-CS filled with liquids was weighed after the removal of excess liquid by filter paper. The adsorbent ability of MTA-CS was calculated by the following equation:

$$Q=\frac{W_1-W_0}{W_0} \tag{2}$$

where Q (g/g) is the oil-sorption capacity defined as gram of adsorbed oil per gram of dried aerogel, W_0 and W_1 are the weight of aerogel before and after absorption in the selected organic solvents or oil, respectively. Each test was repeated three times to obtain an average value.

Water contact angle (WCA) test was carried out to investigate the hydrophobicity of MTA-CS on a contact angle meter (JGW) with a high-speed camera. Water (1 μL) was carefully dropped onto the aerogel surface at room temperature.

Fourier transform infrared (FTIR) spectroscopy spectra were collected in the region of 400-4,000 cm^{-1} (Perkin Elmer, USA). The morphologies of P-CS, A-CS and MTA-CS were explored by scanning electron microscopy (JSM-7800F, Japan). Materials were attached to the sample holders with conductive double side carb on tape and sputter coated with platinum to avoid charging during the test. The elemental analysis was accomplished using the coupled energy dispersive spectrometer (EDS).

The crystalline phase of raw corn straw, P-CS and A-CS was characterized by X-ray diffraction. XRD patterns were recorded using a Rigaku D/MAX-RB diffractor with Cu K_α radiation source operating at 40 KV and 100 mA. The crystallinity of each sample was calculated according to the Segal empirical formula.

Thermal gravimetric analysis (TGA) was carried out on a thermo plus TG-8120 apparatus. Typically, 50 mg of the aerogel was heated from 20 to 700 °C at a rate of 10 °C/min under an N_2 flow of 50 mL/min.

The specific surface areas were measured using BET (Brunauer, Emmett and Teller) method, which was performed at −196 °C on an ASAP 2010 Micromeritics apparatus. Prior to analysis, the samples were outgassed at 300 °C for 3 h under N_2 flow.

RESULTS AND DISCUSSION

1. Characterization

Fig. 1 shows the microstructure of raw corn straw, P-CS, A-CS, MTA-CS and filter paper based aerogel. As shown in Fig. 1(a), the surface of corn straw was tight and smooth, as proposed that cellulose fiber was tightly wrapped by hemicellulose, pectin and lignin. This was in line with the previous reports [31]. The porous and layered structure can be clearly observed on the surface of P-CS as depicted in Fig. 1(b). It indicates the disrupture of straw structure due to the partial removal of lignin and hemicellulose after alkali treatment. Noticeably, the freeze-dried aerogels which were synthesized from filter paper fibers and corn straw presented a three-dimensional (3D) network structure (Fig. 1(c), 1(d)). The results elucidated that porous structure was maintained due to the ice crystals sublimation during the freeze-drying. The A-CS material was further modified with MTMS via a CVD process to improve its hydrophobicity. As shown in Fig. 1(d) and 1(e), the morphologies of A-CS and MTA-CS have a continuously and steadily three-dimensional (3D) porous structure, which was formed by randomly entangled P-CS and filter paper fibers. Herein, hydrophobic modification resulted in a continuous and cloud-like coating (polysiloxane) on corn straw and filter paper fibers (Fig. 1(e)). Additionally, silicon hydroxyl groups generated from hydrolysis reaction of MTMS reagent might react with hydroxyl groups on the surfaces of fibers, so that it was suggested that silanization reaction had no obvious effect on the porous structures of the A-CS (Fig. 1(e)).

Energy dispersive spectrometry (EDS) was conducted to detect chemical components of A-CS and MTA-CS, and the results are presented in Fig. 2. The oxygen (O) peak and the carbon (C) peak streaming from corn straw and filter paper were observed in both A-CS and MTA-CS. In contrast, a new peak corresponding to Si (Fig. 2(b)) evidenced that silanization reaction successfully occurred using MTMS as modified reagent on A-CS.

Thermogravimetry (TGA) and derivative thermo-gravimetry

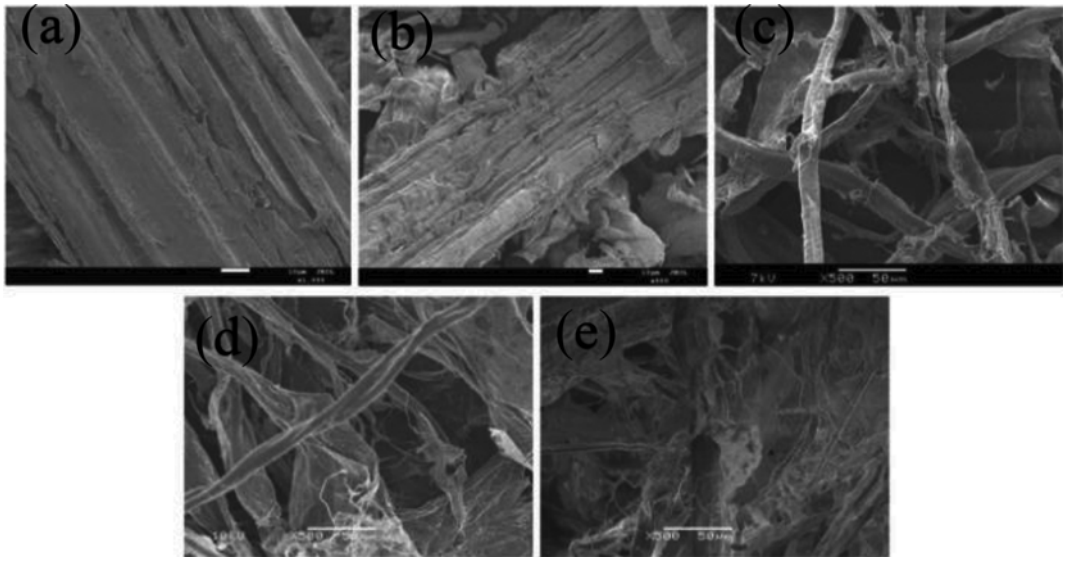

Fig. 1. SEM micrographs of (a) raw corn straw, (b) P-CS, (c) filter paper based aerogel, (d) A-CS, (e) MTA-CS.

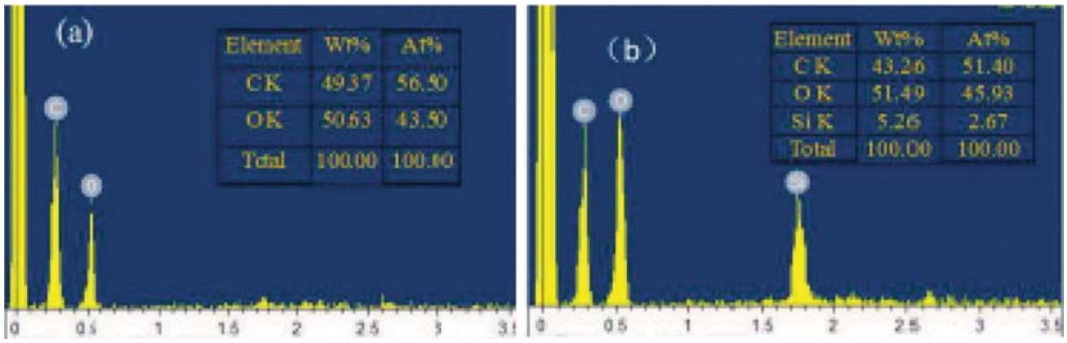

Fig. 2. Energy dispersive spectrometer of (a) A-CS, (b) MTA-CS.

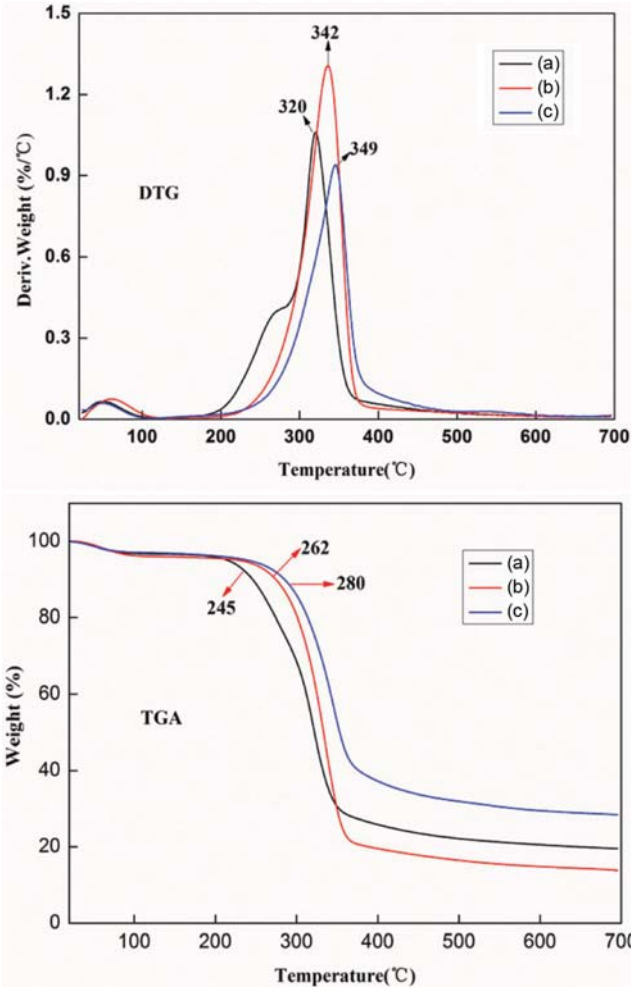

Fig. 3. TGA and DTG thermograms of (a) corn straw, (b) A-CS, (c) MTA-CS under nitrogen atmosphere.

(DTG) results of raw corn straw, A-CS and MTA-CS are shown in Fig. 3. Clearly, only little weight loss occurred in the range of 25-100 °C owing to the evaporation of adsorbed water in all cases. The main weight loss started at 245, 262 and 280 °C for the raw corn straw, A-CS and MTA-CS in TGA, respectively. Moreover, the thermal degradation declined in the following order: corn straw> A-CS>MTA-CS. The degradation process reached its maximum at 320, 342 and 349 °C, respectively, as evidenced in DTG. It indicates that the thermal stability of corn straw was less than the others. It can be concluded that the higher temperature of thermal decomposition was attributed to the removal of lignin from the fibers [30]. Moreover, the residue content of MTA-CS was higher than the values of the raw straw and A-CS at 700 °C. It may be due to the reaction of A-CS and MTMS. Hence, MTA-CS exhibited better thermal stability, making it a promising alternative for application in oil-spill cleanup.

It is known that cellulose crystallinity plays an important role in the mechanical properties. Fig. 4 shows the XRD patterns of the materials to determine the crystallinity. As can be seen, two separate diffraction peaks at ca. 16.5° and 22.5° were assigned to the characteristic bands of cellulose-I crystalline structure [32]. This

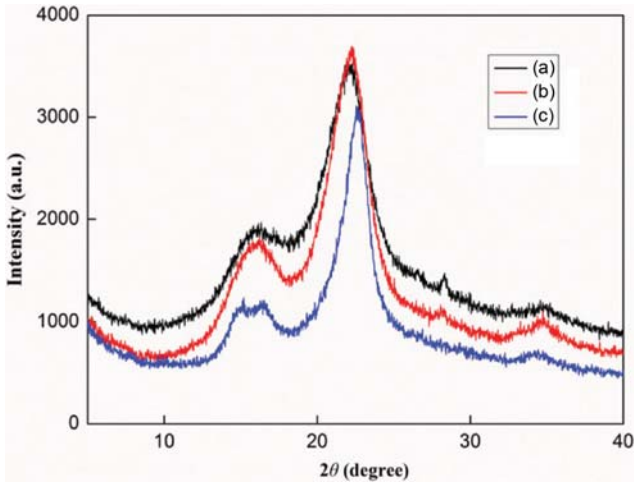

Fig. 4. X-ray diffraction patterns of (a) P-CS, (b) corn straw, and (c) A-CS.

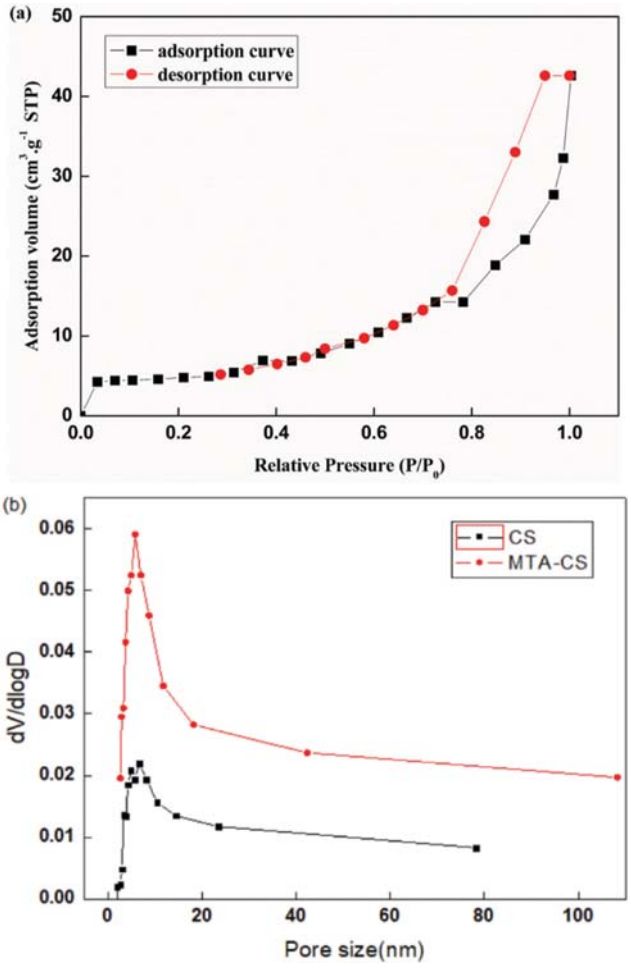

Fig. 5. (a) Nitrogen adsorption and desorption isotherms for MTA-CS, (b) BJH pore size distribution of MTA-CS and corn straw (CS).

indicates that both the alkali treatment and high-shear processing had no influence on the crystal of cellulose. According to Segal

empirical formula [33], the crystallinity values were 45.08, 50.23 and 63.34% for corn straw, P-CS, and A-CS, respectively. Because most of hemicelluloses located in the amorphous regions were removed from the corn straw, the crystallinity of P-CS was increased. Similarly, the increase of crystallinity of A-CS sample caused the filter paper and P-CS to be highly shattered to form homogeneous composite materials. This is in good agreement with the results reported in the previous literature [34,35].

Fig. 5(a) shows the nitrogen sorption isotherm of MTA-CS. Obviously, MTA-CS exhibited a typical type II curve according to the IUPAC classification [36], which presents a characteristic of mesoporous material. The pore diameter distributions were assessed by Barrett-Joyner-Halenda (BJH). As presented in Fig. 5(b), the average pore size of MTA-CS was ca. 17.1 nm, which was less than that of corn straw (22.7 nm), probably because of the addition of filter paper fibers and silylation effect. The result also revealed the partial formation of macropores in all samples (>50 nm), suggesting their hierarchical porous structure. This might be beneficial for oil absorption. Moreover, the measured BET surface areas of MTA-CS and CS materials were 15.42 $m^2 \cdot g^{-1}$ and 3.62 $m^2 \cdot g^{-1}$, respectively. Additionally, fibers from P-CS and filter paper fibers were intertwined together as evidenced by the SEM images (Fig. 1(f)). However, it was difficult to precisely determine the sizes of the formed macropore by nitrogen sorption. In conclusion, MTA-CS was suitable for oil adsorption.

FTIR spectra were conducted to explore the functional groups contained in A-CS and MTA-CS. As presented in Fig. 6, the dominant peaks in the 3,337 cm^{-1}, 1,029 cm^{-1}, 896 cm^{-1} were ascribed to stretching vibrations of -OH, C-O-C and β-glycosidic linkage, respectively [37]. There was no obvious change after methylsilane treatment, indicating that the basic structure of A-CS sample was maintained. Moreover, the absorption bands at 2,967 cm^{-1}, 1,272 cm^{-1} and 779 cm^{-1} corresponded to the stretching vibration of C-H of the methyl group, stretching vibration of Si-C and Si-O-Si asymmetric stretching [38], respectively. After methylsilane process, the -OH groups were replaced by -OSi$(CH_3)_3$ groups from MTMS resulting in the hydrophobic property of the aerogels.

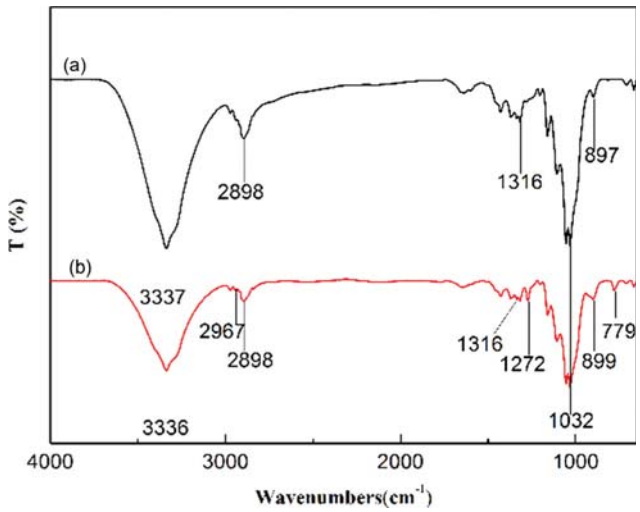

Fig. 6. FT-IR spectra of (a) A-CS, (b) MTA-CS.

Table 1. Physical properties of MTA-CS with different corn straw-filter paper mass ration and concentration

Sample	*m* (P-CS) : *m* (filter paper)	Concentration (%)	Density ($mg \cdot cm^{-3}$)	Porosity (%)
M1	1 : 1	1.0	14±0.15	99.07
M2	1 : 2	1.5	26±0.21	98.29
M3	2 : 1	1.5	35±0.24	97.70
M4	1 : 3	2.0	40±0.21	97.37
M5	1 : 1	2.0	43±0.24	97.17
M6	3 : 1	2.0	48±0.25	96.84
M7	2 : 3	2.5	52±0.29	96.58
M8	3 : 2	2.5	58±0.31	96.18

2. Physical Properties of MTA-CS

Table 1 illustrates the physical properties of MTA-CS. It reveals that the density of aerogels was varied from 14.15 to 58.31 $mg \cdot cm^{-3}$ which was consistent with the previous work on cellulose aerogels [39,40]. The porosity of aerogel could be achieved as high as 99.07%. It was predominantly caused by the increased stacking compactness of fibers, because the crowded fibers significantly reduced the space among fibers. With increasing fiber concentration, P-CS and waste filter paper densely interacted with each other, leading to a robust structure. It was apparent that the fibers might

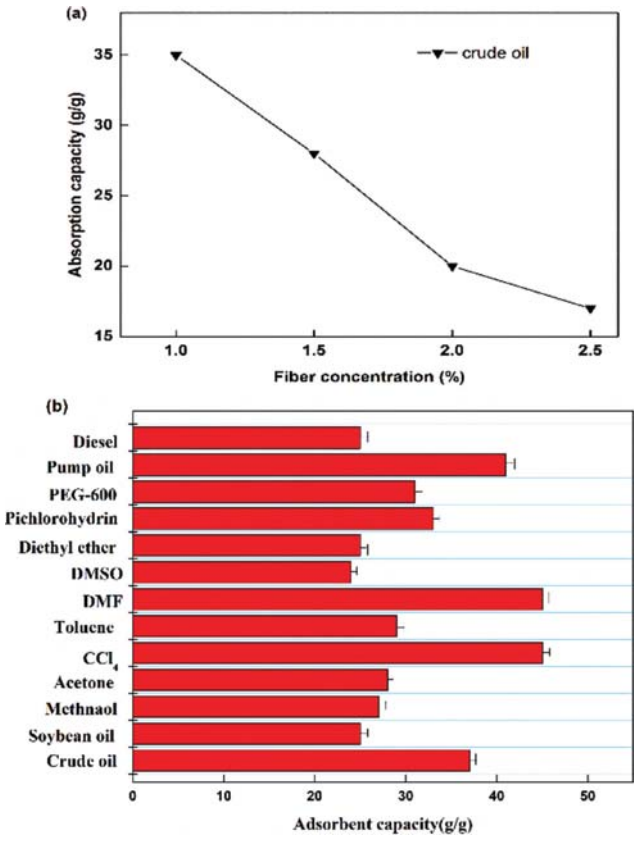

Fig. 7. (a) Effect of fiber concentration on the adsorption capacity for crude oil, (b) adsorption capacity of MTA-CS (1 wt% fiber concentration) for various oils and organic solvents.

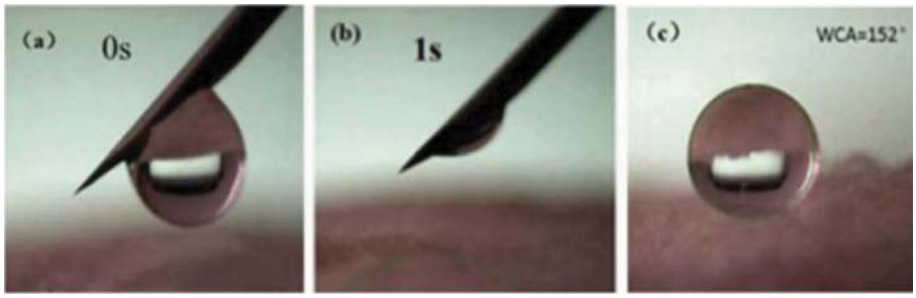

Fig. 8. Images of water contact-angle: (a)-(b) Water droplet on the surface of A-CS, (c) water droplet on the surface of MTA-CS.

easily settle down at a very low fiber concentration (i.e., 0.5%) after high-shear stirring for 30 min. However, increasing fiber concentration to 1% formed a stable and homogeneous suspension because the hydrophilicity on the surface of fibers could significantly enhance the contact between fibers and water, improving the dispersion of fibers. Notably, the density of the as-prepared MTA-CS (14.7 mg·cm^{-3}) was remarkably less than the values of the reported ultralight aerogels and foams, including the carbon aerogel from winter melon (48 mg·cm^{-3}) [41], cellulose-based aerogel (34 mg·cm^{-3}) [42], magnetic shape memory polymer foam (164 mg·cm^{-3}) [43] and cellulose-$CoFe_3O_4$ aerogels (218 mg·cm^{-3}) [44]. Furthermore, the aerogel was light and expected to exhibit high oil absorption capacity. Therefore, MTA-CS with low density could be readily scaled up, because of the facile synthesis method.

3. Oil-sorption Capacity of MTA-CS

The crude oil absorption capacity of MTA-CS was tested, and the results are presented in Fig. 7(a). Interestingly, increasing fiber concentration led to the decline of adsorption capacity. Furthermore, absorption capacities for crude oil increased from 17 to 36 times its own weight upon decreasing fiber concentration from 2.5 wt% to 1 wt%, which might be due to the decreasing density and higher porosity. Therefore, the aerogels with lower density had higher oil absorption capacity. In addition, MTA-CS also exhibited a satisfactory adsorption capacity for other oils (crude oil, pump oil, etc.) and/or organic solvents (CCl_4, DMSO, acetone etc.) as pointed out in Fig. 7(b). It could adsorb as high as 25 to 45 times its own weight. On the contrary, the adsorption capacity of MTA-CS was a little less than those for carbon nanotube [45] and graphene aerogels [46]. However, the preparation procedures for these aerogels are complicated and expensive, which limits their industry applications [47].

Hence, MTA-CS has shown huge potentiality to be used as absorbent for the recovery of spilled oil.

4. Wettability and Oil-water Selectivity

Effective oil/water selectivity is regarded as one of the key factors for oil absorbent [48]. Owing to the large amounts of hydrophilic and hydroxyl groups in corn straw and filter paper, the A-CS cannot be directly used as oil absorption materials.

A-CS was further modified with MTMS in order to achieve high oil-water separation capacity. The wettability of A-CS and MTA-CS was characterized by dynamic contact angle tests of the aerogels surface. As shown in Fig. 8(a)-(b), A-CS exhibits excellent hydrophilicity, the aerogel can absorb water droplet within 1s, and the water contact angle (WCA) is almost 0°. In contrast, MTA-CS presented highly hydrophobic features. Apparently, the water droplet could stand on the surface of MTA-CS and keep its original shape well without obvious penetration within 15 min (Fig. 8(c)). The MTA-CS material exhibits a WCA up to 152°, which is higher than most of the reported hydrophobic natural cellulose materials, such as nanofibers of bacterial cellulose aerogel (BCA) [49], rice straw based cellulose aerogel [50]. As proposed in the previous research on oil absorption aerogels [39,51,52], the surface wettability is greatly controlled by the surface energy and the surface roughness. In this work, the surface energy of MTA-CS decreased after the modification of MTMS, and the formation of the polysiloxane particles on the surface of aerogels endowed the MTA-CS with high surface roughness.

To further demonstrate the adsorption ability and hydrophobicity of MTA-CS, water and oil absorption capability of corn straw, P-CS, A-CS, filter paper and MTA-CS were tested and compared. As shown in Fig. 9, clearly the oil adsorption abilities declined in the following rank: MTA-CS>A-CS>P-CS>corn straw>filter paper. Note that filter paper shows less oil and water absorption ability (3.8 g/g and 2.3 g/g, respectively) compared with other materials, because cellulose fibers in filter paper are closely related to each other. The tight structure of filter paper led to the decrease of surface area and the disappearance of hierarchically porous structure. After the alkali pretreatment, the dense structure of corn straw was destroyed, and the internal fibers were exposed [53]. There-

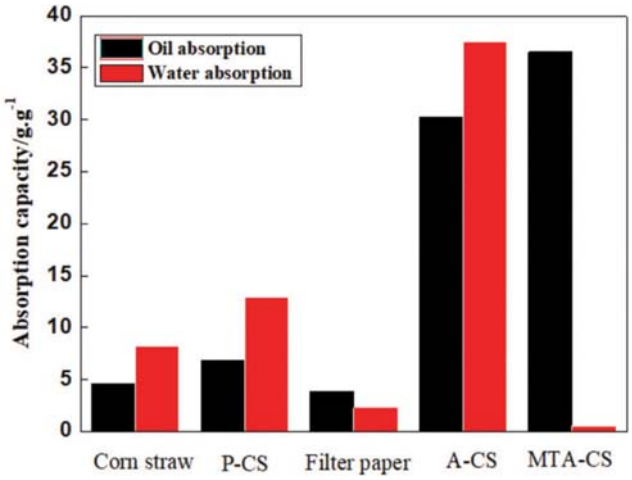

Fig. 9. Water and oil absorption capacities of corn straw, P-CS, filer paper, A-CS and MTA-CS.

fore, the water and oil absorption of P-CS was higher than that of corn straw. Moreover, due to the porous structure of corn straw based aerogel (c), (d), the oil absorption capability of aerogel was significantly higher than the values of corn straw and P-CS. In addition, it was quite clear to know that the oil capacity was 4.6, 6.8 and 30.2 $g \cdot g^{-1}$ for corn straw, P-CS, and A-CS, respectively, corresponding to the water capacity 8.2, 12.9 and 37.5 $g \cdot g^{-1}$ for corn straw, P-CS and A-CS, respectively. The results revealed that corn straw, P-CS and A-CS have poor oil-water selectivity. So, they might be not suitable for application as oil absorbing materials in oil-water separation. In contrast, the oil capacity of MTA-CS reached as high as 36.5 $g \cdot g^{-1}$ and the water capacity was only 0.5 $g \cdot g^{-1}$, which indicates MTA-CS was oleophylic and hydrophobic. In summary, the above discussion suggests that MTA-CS could effectively remove oil spills.

The water-repellency and stability of MTA-CS provided strong potential for its practical application in oil and organic solvents pollution. The low density and porosity of corn straw make it self-floating on the water surface after absorption, which is conducive to the recycling of corn straw [24]. The hydrophobic properties of spongy aerogel based corn straw were investigated. As shown in Fig. 10(a), the crude oil and water (dyed with methyl orange, MOA) rapidly sank into the surface of the aerogel. Both water and oil droplets could be absorbed into A-CS immediately, probably because of the amphiphilic property of cellulose [54,55]. The main component of A-CS and MTA-CS was cellulose. Cellulose has an intrinsically anisotropic molecular structure, the glucopyranose ring in cellulose is hydrophilic, as the three hydroxyl groups located in equatorial positions, whereas the axial direction is hydrophobic due to hydrogen atoms of C-H bonds being in axial positions [55]. So, without any chemical modification, A-CS has poor oil/water selectivity. In contrast, the MTA-CS can support some spherical water droplets on the surface, while crude oil is absorbed very quickly (Fig. 10(b)), demonstrated the superhydrophobic property of the aerogels. Interestingly, the internal surface of MTA-CS also shows high repellency to water (Fig. 10(c)), even when MTA-CS has been cut in half, suggesting that the whole aerogel is hydrophobic. In addition, the element mapping analysis (Fig. 10(d), (e)) revealed the uniform distribution of the Si element over the aerogel surface. This may be due to the high mobility of MTMS in the vapor deposition process and the porous structure of aerogels. Predictably, the silicon hydroxyl groups generated from hydrolysis reaction of MTMS reagent reacted with hydroxyl groups on the surface corn straw and filter paper fibers. [24,56].

In addition, Fig. 11 shows the process of MTA-CS as oil absorbents for the removal of soybean oil from water surface. A mixture of 50 mL water and 5 mL soybean oil was poured into a small

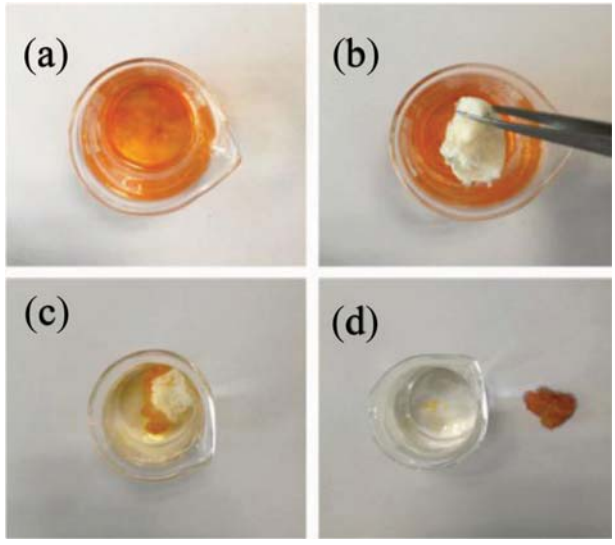

Fig. 11. (a)-(d) Optical images of the removal of soybean oil from the surface of water with MTA-CS.

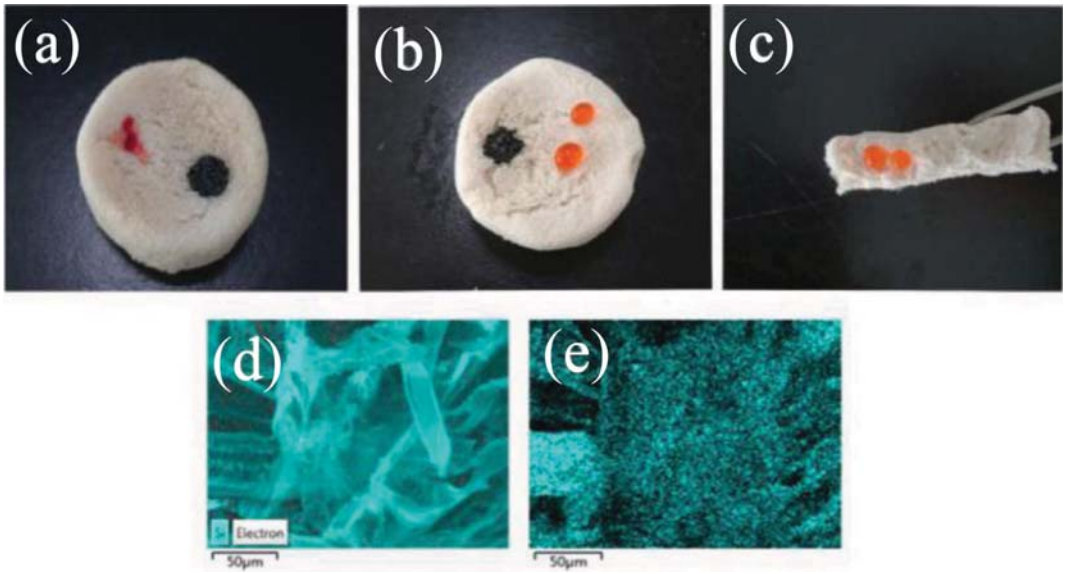

Fig. 10. Photographs of water (dyed with methyl orange) and crude oil(black) on the surface (a) on the surface of A-CS, (b) on the surface of MTA-CS, (c) on the inner section of MTA-CS, (d) and (e) EDS mapping images of MTA-CS.

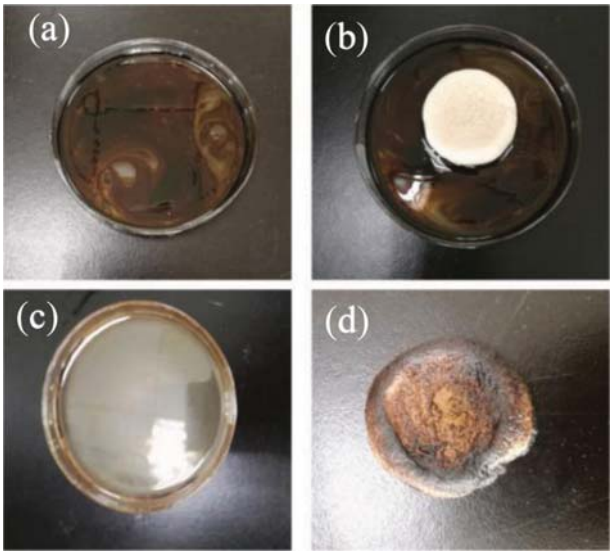

Fig. 12. Photographs of MTA-CS as oil absorbent for removal crude oil from crude oil/water mixture.

beaker and stirred intensely. Then, MTA-CS was dipped into water-oil mixture and the soybean oil layer was completely and rapidly absorbed within 30 s (Fig. 11(a)-(d)). In particular, the flotation of the MTA-CS on the water surface further demonstrated low density and hydrophobicity, in good agreement with the above discussion, indicating its potential use for the facile removal of oils and other organic pollutants.

After successfully removing soybean oil from water, the MTA-CS material was further applied in oil-spill cleanup, which absorbed crude oil from water. To study the oil-spill cleanup behavior of the MTA-CS, a model crude oil/water mixture was obtained by dispersing crude oil into water (Fig. 12(a)). As shown in Fig. 12(b), MTA-CS was immersed into the oil and water mixture, the crude oil was quickly absorbed and the aerogels still floated on the mixture surface even under shaking conditions, exhibiting its low density and hydrophobicity. Finally, the water became clear and transparent within 1 min (Fig. 12(c)) and the aerogel was filled with crude oil (Fig. 12(d)). Obviously, MTA-CS showed an excellent capability to absorb crude oil, which makes it an ideal candidate for oil-spill cleanup.

CONCLUSION

A high hydrophobic spongy aerogel was successfully synthesized using corn straw and waste filter paper as raw materials instead of cost prohibitive materials. The aerogels exhibited several merits such as environment friendliness, high porosity, low-cost and pilot-scale production. Moreover, the adsorption capacity of the MTA-CS for crude oil (above 36 times upon its weight) was higher than that of commercial oil adsorbent, and it was also suitable for a variety of organic solvents. The average water contact angle of MTA-CS was ca. 152°. MTA-CS can quickly remove oils from the water within a short time. Herein, both the relatively cheap raw material and a simply scalable approach made the MTA-CS as a potential alternative in the effective materials for oil spills and chemical leaks clean up. This work will provide an access to the comprehensive utilization of corn straw.

ACKNOWLEDGEMENTS

This work was supported by Liaoning Province Ocean & Fishery office (grant No. 201405), and Dalian Science & Technology Office (grant No. 2015B11NC078).

REFERENCES

1. K. He, H. Duan, G. Y. Chen, X. Y. Liu, W. Yang and D. Wang, *ACS Nano.*, **9**, 9188 (2015).
2. J. Aurell and B. K. Gullett, *Environ. Sci. Technol.*, **44**, 9431 (2010).
3. R. Boopathy, S. Shields and S. Nunna, *Appl. Biochem. Biotechnol.*, **167**, 1560 (2012).
4. S. Jo and Y. Kim, *Korean J. Chem. Eng.*, **11**, 3203 (2016).
5. Y. Li, Z. Wang, L. Yang, X. Li, Y. Zhang and C. Lu, *Ind. Crops Prod.*, **101**, 1 (2017).
6. H. Bi, Z. Yin, X. Cao, X. Xie, C. Tan, X. Huang, B. Chen, F. Chen, Q. Yang, X. Bu, X. Lu, L. Sun and H. Zhang, *Adv. Mater.*, **25**, 5916 (2013).
7. K. Alinezhad, M. Hosseini, K. Movagarnejad and M. Salehi, *Korean J. Chem. Eng.*, **27**, 198 (2010).
8. D. Angelova, I. Uzunov, A. Gigova and L. Minchev, *Chem. Eng. J.*, **172**, 306 (2011).
9. S. J. Choi, T. H. Kwon, H. Im, D. I. Moon and M. L. Seol, *ACS Appl. Mater. Interfaces*, **3**, 4552 (2011).
10. M. Radetic, V. Ilic, D. Radojevic, R. Miladinovic, D. Jocic and J. Jovancic, *Chemosphere*, **70**, 525 (2008).
11. Q. Zhu, Y. Chu, Z. Wang, N. Chen, L. Lin, F. Liu and Q. Pan, *J. Mater. Chem. A*, **1**, 5386 (2013).
12. O. Carmody, R. Frost, Y. Xi and S. Kokot, *Colloid Interface Sci.*, **305**, 17 (2007).
13. Y. Meng, T. M. Young, P. Liu, C. I. Contescu, B. Huang and S. Wang, *Cellulose*, **22**, 435 (2015).
14. M. Khosravi and S. Azizian, *ACS Appl. Mater. Interfaces*, **7**, 25326 (2015).
15. P. Fan, Y. Yuan, J. Ren, B. Yuan, Q. He, G. Xia, F. Chen and R. Song, *Carbohydr. Polym.*, **162**, 108 (2017).
16. Q. Liao, X. Su, W. Zhu, W. Hua, Z. Qian, L. Liu and J. Yao, *RSC Adv.*, **6**, 63773 (2016).
17. C. Yin, J. Lin, Q. Xu, Q. Peng, Y. Liu and X. Shen, *Carbohydr. Polym.*, **67**, 147 (2007).
18. D. G. Raut, O. Sundman, W. Su, P. Virtanen, Y. Sugano, K. Kordas and J. P. Mikkolau, *Carbohydr. Polym.*, **130**, 18 (2015).
19. K. Petzold, A. Koschella, D. Klemm and B. Heublein, *Cellulose*, **10**, 251 (2003).
20. S. Wang, X. Peng, L. Zhong, J. Tan, S. Jing, X. Cao, W. Chen, C. Liu and R. Sun, *J. Mater. Chem. A.*, **3**, 8772 (2015).
21. X. Zhou, P. Wang, Y. Zhang, X. Zhang and Y. Jiang, *ACS Sustainable Chem. Eng.*, **4**, 5585 (2016).
22. J. Wang, A. Wang and W. Wang, *Ind. Crops Prod.*, **108**, 303 (2017).
23. X. Lu, Y. Zhang, Y. Liang, J. Yang, S. Zhang and E. Suzuki, *Korean J. Chem. Eng.*, **25**, 32 (2008).
24. D. Zang, M. Zhang, F. Liu and C. Wang, *J. Chem. Technol. Biotech-*

nol., **91**, 2449 (2016).
25. X. Zhang, Z. Yuan, T. Wang, Q. Zhang and L. Ma, *RSC Adv.*, **6**, 102306 (2016).
26. H. Wang, W. Xia and P. Lu, *Korean J. Chem. Eng.*, **34**, 1867 (2017).
27. C. C. Yoo, N. P. Nghiem and T. H. Kim, *Korean J. Chem. Eng.*, **10**, 2863 (2016).
28. J. Fu, S. Wang, C. He, Z. Lu, J. Huang and Z. Chen, *Carbohydr. Polym.*, **147**, 89 (2016).
29. L. Guo, L. Gong, X. Cheng, C. Li and H. Zhang, *Mater. Design*, **99**, 349 (2016).
30. H. L. Cheng, B. Gu, M. P. Pennefather, T. X. Nguyen and N. Phan-Thien, *Mater. Design*, **130**, 452 (2017).
31. J. Feng, S. T. Nguyen, Z. Fan and H. M. Duong, *Chem. Eng. J.*, **270**, 168 (2015).
32. L. Zheng, Z. Dang, X. Yi and H. Zhang, *J. Hazard. Mater.*, **176**, 650 (2010).
33. M. Martelli-Tosi, O. B. G. Assis, N. C. Silva, B. C. Esposto, M. A. Martins and D. R. Tapia-Blácido, *Carbohydr. Polym.*, **157**, 512 (2017).
34. S. Liu, Q. Yan, D. Tao, T. Yu and X. Liu, *Carbohydr. Polym.*, **89**, 551 (2012).
35. S. Xiao, R. Gao, Y. Lu, J. Li and Q. Sun, *Carbohydr. Polym.*, **119**, 206 (2015).
36. C. W. Kim, D. S. Kim, S. Y. Kang, M. Marquez and Y. L. Joo, *Polym.*, **47**, 5101 (2006).
37. L. C. Segal, J. J. Creely, A. E. Martin and C. M. Conrad, *Textile Res. J.*, **29**, 786 (1959).
38. M. Zhang, F. Wang, R. Su, W. Qi and Z. He, *Biosci. Rep.*, **101**, 4958 (2010).
39. L. Heath and W. Thielemans, *Green Chemistry*, **12**, 1448 (2010).
40. F. Liebner, E. Haimer, M. Wendland, M. A. Neouze, K. Schlufter and P. Miethe, *Macromolecular Bioscience*, **10**, 349 (2010).
41. Y. Q. Li, Y. A. Samad, K. Polychronopoulou, S. M. Alhassan and K. Liao, *ACS Sustainable Chem. Eng.*, **2**, 1492 (2014).
42. H. Zhang, Y. Li, Y. Xu, Z. Lu, L. Chen, L. Huang and M. Fan, *Phys. Chem. Chem. Phys.*, **18**, 28297 (2016).
43. G. Vialle, M. D. Prima, E. Hocking, K. Gall, H. Garmestani, T. Sanderson and S. C. Arzberger, *Smart Mater. Struct.*, **18**, 115014 (2009).
44. J. Wei, D. Zhou, Z. Sun, Y. Deng, Y. Xia and D. Zhao, *Adv. Funct. Mater.*, **23**, 2322 (2013).
45. Y. Zhao, C. Hu, Y. Hu, H. Cheng, G. Shi and L. Qu, *Angew. Chem. Int. Ed.*, **51**, 11371 (2012).
46. X. Gui, J. Wei, K. Wang, A. Cao, H. Zhu, Y. Jia, Q. Shu and D. Wu, *Adv. Mater.*, **22**, 617 (2010).
47. S. Zhou, P. Liu, M. Wang, H. Zhao, J. Yang and F. Xu, *ACS Sustainable Chem. Eng.*, **4**, 6409 (2016).
48. X. Yu, S. Tong, M. Ge, L. Wu, J. Zuo, C. Cao and W, Song, *J. Environ. Sci.*, **25**, 936 (2015).
49. H. Sai, R. Fu, L. Xing, J. Xiang, Z. Li, F. Li and T. Zhang, *ACS Appl. Mater. Interfaces*, **7**, 7373 (2015).
50. F. Jiang and Y. L. Hsieh, *J. Mater. Chem. A*, **2**, 6337 (2014).
51. Y. Si and Z. Guo, *Nanoscale*, **7**, 5922 (2015).
52. Y. Yang, H. Yi and C. Wang, *ACS Sustainable Chem. Eng.*, **3**, 3012 (2015).
53. T. Zhai, Q. Zheng, Z. Cai, H. Xia and S. Gong, *Carbohydr. Polym.*, **148**, 300 (2016).
54. D. M. Rein, R. Khalfin and Y. Cohen, *J. Colloid Interface Sci.*, **386**, 456 (2012).
55. S. Wang, M. Li and Q. Lu, *ACS Appl. Mater. Interfaces*, **2**, 677 (2010).
56. X. Zhou, Z. Zhang, X. Xu, X. Men and X. Zhu, *Ind. Eng. Chem. Res.*, **52**, 9415 (2013).